UNIVERSITEIT VAN PRETORIA
UNIVERSITY OF PRETORIA
YUNIBESITHI YA PRETORIA

Possible Effect of Hydraulic Fracturing On Seismic Hazard in South Africa

BY:

Prof. Andrzej Kijko (Pr.Sci.Nat), Ansie Smit
University of Pretoria Natural Hazard Centre, Africa
University of Pretoria
Cnr Lynnwood Road and Roper Street
Pretoria
0002
South Africa
andrzej.kijko@up.ac.za, ansie.smit@up.ac.za

PREPARED FOR:

Water Research Commission Project K5/2149

Development of an interactive vulnerability map and preliminary screening level monitoring protocol to assess the potential environmental impact of hydraulic fracturing.

UNIVERSITEIT VAN PRETORIA
UNIVERSITY OF PRETORIA
YUNIBESITHI YA PRETORIA

CONTENTS

List of Figures

List of Tables

Executive Summary

The aim of this report is to portray the current seismic hazard as well as to estimate the possible effect of increased seismic activity due to the planned hydraulic fracturing in South Africa. The seismic hazard is expressed in terms of four maps. Each of these maps portrays different potential effects of hydraulic fracturing. This is done by indicating the value of the peak ground acceleration (PGA) which is expected, with a 10% probability, to be exceeded at least once within 50 years. Based on current knowledge of the geology and tectonic setting of South Africa, it is impossible precisely predict if, and by how much the hydraulic fracturing will lead to an increase the seismic hazard of South Africa. The following four scenarios were therefore considered: a) no increase of seismicity, as well as where seismicity increases b) 2 times, c) 5 times and in the extreme case, d) 10 times. The respective scenarios are illustrated in Maps No. 1 to No. 4. Map No. 5 represents the estimated seismic hazard in South Africa when taking into account the above four possible scenarios which hydraulic fracturing may have on the seismicity. To assess the expected effect of hydraulic fracturing on seismic hazard in South Africa, a formalism in the form of a logic tree was applied. It was assumed that the logic tree weights (l_w) of the four scenarios are 0.15, 0.50, 0.30 and 0.05 respectively. It has to be strongly emphasized that these weights (l_w) are very subjective; it was selected according to a wide scatter and often contradicting expert opinions on the effect of hydraulic fracturing on seismicity. These opinions are available in the current respective literature (e.g. Davis and Frohlich, 1993; De Pater and Baisch 2011; Davies *et al*., 2013; Green *et al*., 2012; Horton,2012; King, 2010; Maxwell *et al*., 2009; Suckale, 2009; Zoback and Harjes, 1997).

Comparison of these five maps suggest that the introduction of hydraulic fracturing in South Africa can/will lead to high levels of seismic hazard in the parts of the Western Cape, the Free State, Gauteng and towards the eastern border of the North West Province. Moderate hazard levels can be expected in the Limpopo Province and parts of the Northern Cape. The southern part of the Eastern Cape is subject to low levels of seismic hazard.

For the purpose of this report the associated hazard (peak ground acceleration) is set equivalent to vulnerability as defined in UNISDR (2004). This report defines vulnerability as the conditions determined by physical, social, economic and environmental factors or processes, which increase the susceptibility of a community to the impact of hazards.

A more reliable assessment of the effect of hydraulic fracturing on seismic hazard in South Africa can be achieved only through the inclusion of detailed geological and tectonic information about the area.

Section 1 provides an introduction and is followed by a brief description on the tectonic setting (Section 2) and seismicity (Section 3) of South Africa. The applied procedure for the computation of the probabilistic seismic hazard maps are described in Section 4. Section 5 provides the description on the input data used with the results described in Section 6. A monitoring protocol for seismic hazard is discussed in Section 7. A brief description of the possible impact of hydraulic fracturing is available in Appendix B.

1. Introduction

Seismic activity in South Africa can be divided into two major groups, the predominantly mining related seismicity as well as seismicity of natural (tectonic) origin. In this report the term seismic event refers to both natural and mining-related events. The associated seismic hazard, the physical effects of a seismic event, is of great importance to the engineering, insurance and disaster management industries. Seismic hazard is typically characterized by phenomena such as surface faulting, ground shaking and liquefaction. For the purposes of this report, the seismic hazard is expressed in terms of the likelihood to observe the maximum acceleration of the ground shaking during a seismic event namely peak ground acceleration (PGA). This acceleration is expressed in units of g, where g is equal to 9.81 m/s^2.

Five maps were created to assess the potential effect of hydraulic fracturing in the South African environment. This was done under the assumption that the hydraulic fracturing process will cause induced seismicity, which in turn could result in an increase in the seismic activity rate. Map No. 1 portraits the current seismic hazard in South Africa, expressed in terms of PGA with (10% probability of exceedance at least once within in 50 years). The map was calculated for the current value of the

mean seismic activity rate λ, i.e. $c_f = 1$. The correcting factor c_f is applied to the seismic activity rate λ to indicate the factor by which the activity rate is increased for the four possible scenarios i.e. a) no increase of seismicity and seismicity increases b) 2 times, c) 5 times and d) 10 times. Maps No. 2 to 4 respectively represent the 10% probability of exceeding the expected peak ground acceleration (PGA) at least once in 50 years for activity rates with the respective correcting factors $c_f = 2$, 5 and 10. These maps are available in Section 6. Finally, Map No. 5 represents the expected seismic hazard in South Africa after taking into account the four possible scenarios of the effect of hydraulic fracturing. To assess the expected effect of hydraulic fracturing on seismic hazard in South Africa, the assessment was performed by the application of the logic tree formalism through the association of the respective logic tree weights (l_w = 0.15, 0.50, 0.30 and 0.05) with the above four scenarios.

These maps provide a convenient tool to estimate the expected seismic risk and response to seismic event loading for different types of structures and buildings located in the South African provinces. By combining these maps with additional geological information, they could also be used as an aid in seismic hazard mitigation.

At least two similar investigations of seismic hazard in South Africa, as presented in Map No.1, were compiled in the past. In 1992, L.M Fernandez and A. du Plessis produced "Seismic Hazard Maps of Southern Africa" (Fernandez and du Plessis, 1992) and in 2003 Kijko *et al*, (2003) published the interactive CD "Probabilistic Peak Ground Acceleration and Spectral Seismic Hazard Maps for South Africa". This map by Kijko *et al*., (2003) is implemented into the South African Building Code SABS (2009). More details regarding the applied theory are available in the discussion of the map creation process in Section 4.

2. The tectonic setting of South Africa

(based on Kijko *et al.*, 2003)

The first recorded seismic phenomenon in South Africa was reported in 1620 by the early Dutch settlers. The improvement in the recording methods of seismic events as well as investigations into the seismic nature of South Africa indicated that the area behaves typically of an intraplate region. An intraplate region is usually characterised by low-level seismic activity, compared to world standards, with seismic events randomly distributed in both space and time. However, the correlation

between seismic event location and the surface expression of major geological features is not clear (Fernandez and Guzman, 1979 a and b).

The African plate, on which South Africa is situated, consists of the East African Rift System, southern Africa and ends in the Indian Ocean. Plate boundaries in both the continental and oceanic lithosphere (including the African wide-plate boundary) are hundreds and thousands of kilometres wide, and in fact cover roughly 15% of Earth's total surface area (Gordon and Stein, 1992).

Maps of the residual bathymetry in the ocean basins around the African continent were investigated by Nyblade and Robinson (1994) and found a broad bathymetric swell in the south-eastern Atlantic Ocean, with amplitude of about 500 m. This region of anomalously shallow bathymetry together with the contiguous eastern and southern African plateaus, form a superswell log of which the origin is uncertain. The authors speculate that it may be partly attributed to the heating of the lithosphere which caused rifting and volcanism in eastern Africa and is indicated by high heat-flow measurements in southern Africa and the south-eastern Atlantic Ocean. This theory is supported by Su *et al*., (1994) and Grand *et al*., (1997), who respectively constructed a three-dimensional shear wave velocity model as well as shear wave and pressure wave velocity heterogeneity models of the Earth's mantle from an inversion of a large set of seismic travel time data. Both investigations found evidence for the existence of large mega-structures with associated anomalous velocities in the Earth. Su *et al*., (1994) interpret the velocity anomaly, found under part of Africa, as hot mantle material in the depth interval of 800 to 2300 km.

Evidence of tectonic uplift in southern Africa during the last 3 Ma (mega-annum) may be inferred from the uplift of Neogene diamond-bearing marine deposits and the relationship between onshore denudation and offshore sedimentation in, for example, KwaZulu Natal (Hartnady and Partridge, 1995). These authors subsequently speculated that the diapir plumes that buoy up a large part of East Africa have also affected South Africa. The African wide-plate boundary is characterised by belt-like zones of seismicity surrounding relatively aseismic blocks. The seismicity in South Africa appears to portray the same spatial style and supports the notion that the wide-plate boundary extends into South Africa. The rift between the Nubia and the Somalia plates, south of 20^{o} S off the coast of Mozambique, is along the southwest Indian Ridge (Lemaux *et al*., 2002). Hence, even though South Africa may be influenced by the wide-plate boundary, the rift itself does not extend into the country.

3. A brief description of South African seismicity

(based on Kijko *et al.*, 2003)

The highest natural seismic activity, where the peak ground acceleration (PGA) exceeds 0.05 g, as per the commentary on the Seismic Hazard Map in the SABS Code of Practise manual of 1994 (SABS, 1994), is observed in the south-eastern Cape and around Lesotho. In the past, PGAs of 0.39 g and 0.45 g have been recorded for the deep gold-mining areas of Klerksdorp and Carletonville (SABS, 1994).

Evidence that has emerged from deep gold mines in South Africa indicate that mining-induced seismicity is characterised by normal faulting due to stope closure and that tectonic stresses play an insignificant role (Dennison and Van Aswegen, 1993; Wong, 1993). The bulk of the seismic events recorded and located by the South African National Seismograph Network (SANSN; Saunders *et al.*, 2008) are attributed to mine tremors due to the deep gold-mining operations around the Witwatersrand basin area. The gold-bearing reefs of the Witwatersrand system are mined by stoping at depths reaching ± 3.5 km (Gibowicz and Kijko, 1994; Gibowicz and Lasocki, 2001). The local networks of geophones, installed in many of the gold mines, record the seismic events with greater accuracy than that obtained from the SANSN.

A study of a few recent mining-induced seismic events in South Africa (1999 to 2005) indicates that in the gold-mining area of Klerksdorp (eastern North West Province) seismic events of local Richter magnitudes M_L up to 5.3 were recorded. In the Koffiefontein diamond mining area in the Free State, three events of local magnitudes M_L between 2.7 to 4.5 were recorded during June and July 1999. The largest mining-related seismic event in South Africa occurred on 9 March 2005 in the Stilfontein mining-area (Figure 1) between Potchefstroom and Klerksdorp (M_L=5.3) in 2005. Several buildings in the town were damaged by this event.

However the strongest and most devastating South African seismic events of the 20th century are attributed to the natural seismicity in the Western Cape. The Ceres-Tulbagh seismic event of 29 September 1969, with local Richter magnitude 6.3, is the largest recorded event. This event was felt widely over the Western Cape, especially at Ceres, Tulbagh and Wolseley. Several buildings in the area suffered serious damage, varying from the almost total destruction of old and also poorly built buildings, to large cracks appearing in those that were better constructed (Figure 2). Twelve people were killed and many more injured. This event had an insured loss of US$7.4 million (approximately

R75 million at today's exchange rates). However the uninsured loss was roughly 3.5 times higher (AXCO (unpublished)).

The magnitude 6.0 to 6.5 seismic event that occurred off Cape St Lucia on 31 December 1932 caused damage to poorly constructed buildings, with one or two collapsing. Cracks and fissures in the ground were also reported.

On 8 December 1976 a seismic event of magnitude 5.2 occurred in Welkom. There was extensive damage to many buildings, the most dramatic of which was the collapse of a six-story high block of flats, which took place 75 minutes after the event (Figure 3).

In the Carletonville area in the North West Province, a seismic event of magnitude 4.7 occurred on 7 March 1992. An unusual amount of damage was recorded, owing to the high population density around the epicentral area. Houses were damaged as far as Pretoria (ca. 100 km away).

Figure 1: Effect of the 2005 Stilfontein seismic event of M_L 5.3 on the A-block of the Bal-Eaton flats. (Photo courtesy of Ian Saunders, Council for Geoscience, Pretoria)

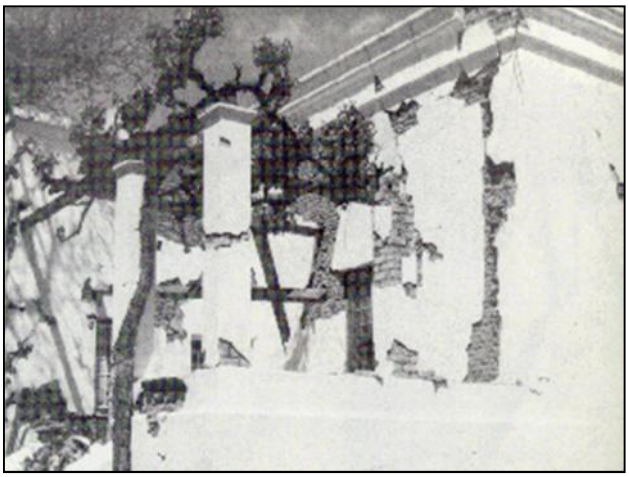

Figure 2: Illustration of the damage to an old building in Ceres owing to the seismic event of 29 September 1969. "The damage at Drostdy was spectacular because the buildings in the hamlet were of the older types of construction. The high Cape-Dutch gables of these older buildings were particularly susceptible to damage. The historic Drostdy (Magistrate's residence) was constructed partly of sun-dried brick and partly of brick, with clay as mortar. The damage to this beautiful old building was very serious as neither type of masonry could resist the severe seismic shaking. Most of the cracks in the walls were caused by oscillation of the walls, as is evidence by the vertical cracks in the corners and the diagonal cracks in the walls" (Van Wyk and Kent, 1974).

Figure 3: The 1976 Welkom seismic event in which a block of flats, six storeys high, collapsed. (Photographer unknown)

4. Applied procedure for the computation of probabilistic seismic hazard maps

4.1. Problem Formulation

The essence of the probabilistic seismic hazard analysis (PSHA) is the calculation of the probability of exceedance of a specified ground motion level at a specified site (Cornell, 1968; Reiter, 1990). In principle, PSHA can address a very broad range of natural hazards associated with seismic events, including ground shaking and ground rupture, landslide, liquefaction or tsunami. However, in most cases the interest of designers lies in the estimation of the likelihood of a specified level of ground shaking, since it causes the greatest economic losses.

The typical output of the PSHA is the seismic hazard curve (often a set of seismic curves), i.e. plots of the estimated probability, per unit time, of the ground motion variable, e.g. peak ground acceleration (PGA) being equal to or exceeding the level as a function of PGA (Budnitz *et al*., 1997). The essence of the PSHA is that its product – the seismic hazard curve, quantifies the hazard at the site from all possible seismic events of all possible magnitudes at all significant distances from the site of interest, by taking into account their frequency of occurrences. In addition to the hazard curve, the output of PSHA includes results of the so called de-aggregation procedure. This procedure provides information on seismic event magnitudes and distances that contribute to the hazard at a specified return period and at a structural period of engineering interest (Budnitz *et al*., 1997).

In general, the standard PSHA procedure is based on two sources of information: (1) observed seismicity, recapitulated by seismic event catalogue, and (2) area-specific, geological data (e.g. a regional seismotectonic model of the area). After the combination of a selected model of seismic event occurrence with the information on the regional seismic wave attenuation or ground motion prediction equation (GMPE), a regional seismotectonic model of the area is formulated and an assessment of the seismic hazard is performed. Detailed investigation into the site effect, determined by site specific soil properties, should be done to improve the accuracy of the PGA. Complete PSHA can be carried out only when information on the regional seismotectonic model and the site-specific soil properties are known.

Clearly, all the above information required to complete PSHA is subjective and often highly uncertain, especially in stable continental areas where the seismic event activity is very low.

According to the convention established in the fundamental document by Budnitz *et al*., (1997) there are two types of uncertainties associated with PSHA: aleatory and epistemic.

According to Budnitz *et al*., (1997) the uncertainties that are part of the applied model used in the analysis are called aleatory uncertainties. The other names for the aleatory uncertainty are 'stochastic' or 'random' uncertainties. Even when the model is perfectly correct and the numerical values of its parameters are known without any errors, aleatory uncertainties for a given model are still present (Budnitz *et al*., 1997).

The uncertainties which come from incomplete knowledge of the models, i.e. when wrong models are applied or/and the numerical values of their parameters are not known, are called epistemic uncertainties. As relevant information is collected, the epistemic uncertainties can be reduced (Budnitz *et al.*, 1997).

By the definition of the PSHA procedure, the aleatory uncertainty is included in the process of PSHA calculations by means of applied models (statistical distributions) and by mathematical integration. Epistemic uncertainty can be incorporated in the PSHA by the consideration of an alternative hypotheses (e.g. alternative boundaries of the seismic sources and their recurrence parameters) and alternative models (e.g. alternative seismic event distributions or/and application of alternative PGA attenuation equations). Incorporation of this type of uncertainties into the PSHA is carried out by the application of the logic tree formalism. A complete PSHA includes an account of aleatory as well as epistemic uncertainties. Any PSHA without the incorporation of the above uncertainties is considered to be incomplete.

This following section describes two major mathematical aspects of the PSHA:

(1) The procedure for the assessment of the seismic source characteristic recurrence parameters when the data are incomplete and uncertain. Use is made of the most common assumptions in engineering seismology i.e. the seismic event occurrences in time follow a Poisson process and that seismic event magnitudes are distributed according to a Gutenberg-Richter doubly-truncated distribution. Following the above assumptions, the seismic source recurrence parameters are defined as (a) the mean seismic activity rate λ (which is a parameter of the Poisson distribution), (b) the level of completeness of the seismic event catalogue $m_{\min}$, (c) the maximum regional seismic event magnitude $m_{\max}$ and (d) the Gutenberg-Richter parameter b. To assess the above parameters a seismic event catalogue containing origin

times, size of seismic events and spatial locations are needed. The maximum seismic source characteristic event magnitude $m_{\max}$ is of paramount importance in this approach; therefore a statistical technique that can be used for evaluating this important parameter is presented in Section 4.2.6.

(2) PSHA methodology i.e. calculating the probability of exceedance of a specified ground motion level at a specified site. Often, the presented approach is known as the Cornell-McGuire procedure. The essence of the Cornell-McGuire PSHA procedure is the calculation of the probability of exceedance of a specified ground motion level at a specified site. The so called Cornell-McGuire solution of this problem consists of four steps: (e.g. Budnitz *et al*., 1997; Reiter, 1990):

- determination of the possible seismic sources around the site.
- determination and assessment of the recurrence parameters for each seismic source.
- selection of the ground motion prediction equation (GMPE) which is most suitable for the region.
- computation of the hazard curves.

4.2. Probabilistic Seismic Hazard Assessment – Theoretical Background

This section provides an outline of the procedure used to determine the seismic source recurrence parameters: the area characteristic mean seismic activity rate λ, the Gutenberg-Richter parameter b, the level of completeness of the seismic event catalogue $m_{\min}$ and the maximum regional seismic event magnitude $m_{\max}$.

4.2 1. Nature of input data

The lack or incompleteness of data in seismic event catalogues is a frequent issue in the statistical analysis of seismic hazard. Contributing factors include the historical and socio–economic context, demographic variations and alterations in the seismic network. Generally, the degree of completeness is a monotonically increasing function of time i.e. the more recent portion of the catalogue has a lower level of completeness. The methodology makes provision for the seismic

event catalogue to contain three types of data (Kijko and Sellevoll, 1989; 1992). Figure 4 depicts the typical scenario confronted when conducting seismic hazard assessments:

- very strong prehistoric seismic events (paleo-earthquakes) which usually occurred over the last thousands of years,
- the macro-seismic (historic) observations of some of the strongest seismic events that occurred over a period of the last few hundred years,
- complete recent data for a relatively short period of time.

The complete part of the catalogue can be divided into several sub-catalogues each of which is complete for events above a given threshold magnitude $m_{\min}^{(i)}$, and occurring in a certain period of time T_i where $i = 1, \ldots, S$ and S is the number of complete sub-catalogues. The approach permits 'gaps' (T_g) when records were missing or the seismic networks were out of operation. The procedure is capable of accounting for uncertainties of occurrence time of prehistoric earthquakes. Uncertainty in seismic event magnitude is also taken into account through the assumption that the observed magnitude is the true magnitude subjected to a random error. It is further assumed that the random error follows a Gaussian distribution having zero mean and a known standard deviation.

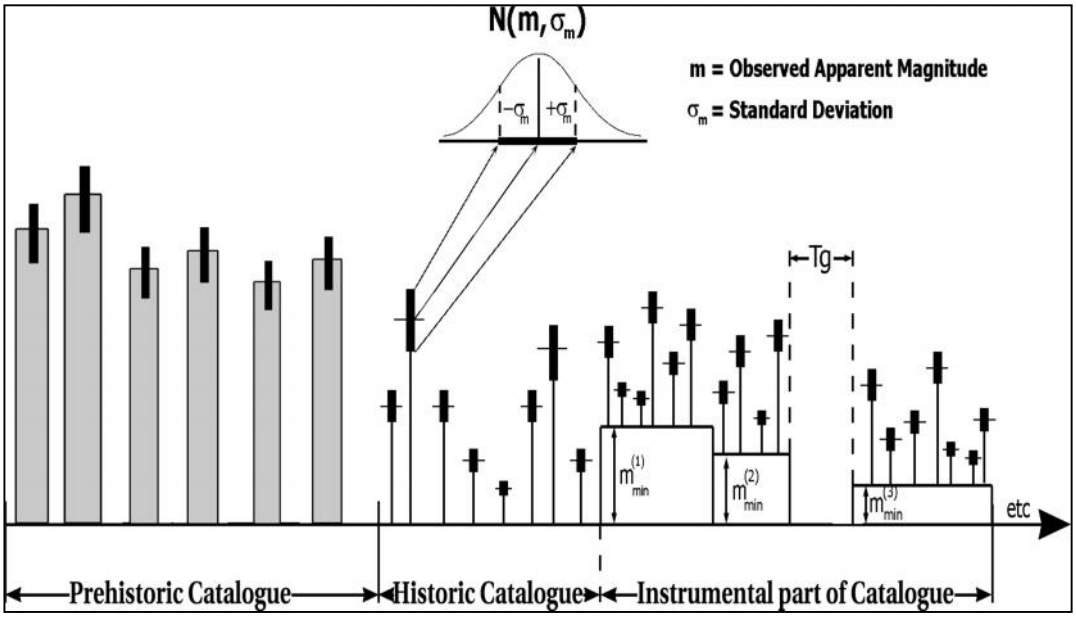

Figure 4: Illustration of data which can be used to obtain reccurence parameters for the specified seismic source. (Modified after Kijko and Sellevoll, 1992)

4.2.2. Statistical preliminaries

Basic statistical distributions and quantities utilized in the development of the methodology are briefly described in this section.

The Poisson distribution is used to model the number of occurrences of a given seismic event magnitude or a given amplitude of a selected ground motion parameter being exceeded within a specified time interval.

$$p(n|\lambda,t) \equiv P(N=n|\lambda,t) = \frac{(\lambda t)^n}{n!}e^{-\lambda t}, \qquad n = 0,1,2 \ldots \tag{1}$$

Note that λ here refers to the parameter of the Poisson distribution and describes the area characteristic, mean activity rate (mean number of occurrences within specified time interval, usually 1 year).

The Gamma distribution, given its flexibility, is used to model spatial and temporal fluctuation (uncertainty) of various seismic hazard parameters and it's the distribution is given by

$$f(x) = x^{(q-1)}\frac{p^q}{\Gamma(q)}e^{-px}, \qquad x > 0 \tag{2}$$

where $\Gamma(q)$ is the Gamma function defined as

$$\Gamma(q) = \int_0^\infty y^{q-1}e^{-y}dy, \quad q > 0 \tag{3}$$

The parameters p and q are related to the mean μ and the variance σ^2 of the distribution according to

$$\mu^x = \frac{q}{p} \tag{4}$$

$$\sigma_{\bar{x}}^2 = \frac{d}{p^2}. \tag{5}$$

The coefficient of variation expresses the uncertainty related to a given parameter and is given by

$$COV_x = \frac{\sigma_x}{\mu_x}, \tag{6}$$

thus describing the variation of a parameter relative to its mean value. A higher value indicates a greater dispersion of the parameter.

4.2.3. Estimation of the seismic source recurrence parameters

The standard assumption adopted is that the distribution of number of seismic events, with respect to their size, obeys the classic Gutenberg-Richter relation

$$\log N(m) = a - b(m - m_{\min}), \tag{7}$$

where $N(m)$ is the number of seismic events of $m \geq m_{\min}$, occurring within a specified period of time, and a and b are parameters.

Aki (1965) found that equation (7) is equivalent with the assumption that the cumulative distribution function (CDF) of seismic event magnitude is of the form

$$F_M(m) = P(M \leq m) = 1 - e^{-\beta(m - m_{\min})} \tag{8}$$

where $\beta = b\ln(10)$.

The seismic event occurrences over time in the given area are assumed to satisfy a Poisson process (1) having an unknown mean seismic activity rate λ.

The disregard of temporal and spatial variations of the parameters λ and b can lead to biased estimates of seismic hazard. An explicit assumption behind most hazard assessment procedures is that parameters λ and b remain constant in time. However, closer examination of most seismic

event catalogues indicates that there are temporal changes of the mean seismic activity rate λ as well as of the parameter b. For some seismic areas, the b-value has been reported to change (decrease/increase) before large seismic events. Usually, such changes are explained by the state of stress; the higher the stress, the lower the b-value (Gibowicz and Kijko, 1994). Other theories connect the b-value with the homogeneity of the rock: the more heterogeneous the rock, the higher the b-value. Finally, some scientists connect the fluctuation of the b-value with the seismicity pattern and believe that the b-value is controlled by the buckling of the stratum. Whatever the mechanism, the phenomenon of space-time b-value fluctuation is unquestionable and well-known. A wide range of international opinions concerning changes of patterns in seismicity, together with an extensive reference list, are found in a monograph by Simpson and Richards (1981) and in two special issues of Pure and Applied Geophysics, (Seismicity Patterns …, 1999; Microscopic and Macroscopic …, 2000). Treating both parameters λ and b as random variables modelled by respective Gamma distributions allows for appropriately accounting for the statistical uncertainty in these important parameters. In practice, the adoption of the Gamma distribution does not really introduce much limitation, since the Gamma distribution can fit a large variety of shapes.

After combining the Poisson distribution (1) and the Gamma distribution (2), with parameters p_λ and q_λ, the probability to observe n seismic events per unit time t, for randomly varying seismicity, takes the form of the compound distribution

$$P(n|t) = \int_0^\infty P(n|\lambda,t) f(\lambda)\, d\lambda$$
$$= \frac{\Gamma(n+q_\lambda)}{n!\,\Gamma(q_\lambda)} \left(\frac{p_\lambda}{t+p_\lambda}\right)^{q_\lambda} \left(\frac{t}{t+p_\lambda}\right)^{n} \qquad (9)$$

where $p_\lambda = \bar{\lambda}/\sigma_\lambda^2$, $q_\lambda = \bar{\lambda}^2/\sigma_\lambda^2$ and $\Gamma(\cdot)$ is the Gamma function (3). Parameter $\bar{\lambda}$ denotes the mean value of the activity rate λ.

It has to be noted that in statistical literature the compound distributions like (9), arise from many probabilistic models applied in the engineering (Hamada *et al.*, 2008), insurance and risk industries (Klugman *et al.*, 2008). The first application of the compound distributions in seismic hazard assessment was probably done by Benjamin (1968) followed by Campbell (1982, 1983).

Similarly to the procedure followed in obtaining distribution (9), the compound cumulative distribution function (CDF) of seismic event magnitudes are derived by combining the exponential distribution (8) with the Gamma distribution for β with parameters p_β and q_β, and normalizing upon introducing an upper limit $m_{\max}$. This compound CDF of seismic event magnitudes is expressed as (e.g. Campbell, 1982)

$$F_M(m|m_{\min}) = C_\beta \left[1 - \left(\frac{p_\beta}{p_\beta + m_{\max} - m_{\min}}\right)^{q_\beta}\right], \tag{10}$$

where $p_\beta = \bar{\beta}/\sigma_\beta^2$ and $q_\beta = \bar{\beta}^2/\sigma_\beta^2$. The symbol $\bar{\beta}$ denotes the mean value of parameter β, σ_β denotes the standard deviation of a $\bar{\beta}$ and the normalizing coefficient C_β is given by

$$C_\beta = \left[1 - \left(\frac{p_\beta}{p_\beta + m_{\max} - m_{\min}}\right)^{q_\beta}\right]^{-1}. \tag{11}$$

Noting that $q_\lambda = \bar{\lambda} p_\lambda$ and $q_\beta = \bar{\beta} p_\beta$, equations (9) and (10) may respectively be written in an alternative form as

$$P(n|t) = \frac{\Gamma(n + q_\lambda)}{n!\,\Gamma(q_\lambda)} \left(\frac{q_\lambda}{\bar{\lambda}t + q_\lambda}\right)^{q_\lambda} \left(\frac{\bar{\lambda}t}{\bar{\lambda}t + q_\lambda}\right)^{n}, \tag{12}$$

$$F_M(m|m_{\min}) = C_\beta \left[1 - \left(\frac{q_\beta}{q_\beta + \bar{\beta}(m - m_{\min})}\right)^{q_\beta}\right], \tag{13}$$

$$C_\beta = \left[1 - \left(\frac{q_\beta}{q_\beta + \bar{\beta}(m_{\max} - m_{\min})}\right)^{q_\beta}\right]^{-1}, \tag{14}$$

where $q_\beta = \left(COV_\beta^{-1}\right)^2$ and $q_\lambda = \left(COV_\lambda^{-1}\right)^2$. Upon specification of the COV, the parameters $\bar{\lambda}$ and $\bar{\beta}$, referred to as hyper-parameters of the respective distributions, are estimated by applying the maximum likelihood procedure to the observed data.

4.2.4. Extreme magnitude distribution as applied to prehistoric (paleo) and historic events

The likelihood function of the desired seismicity parameters $\boldsymbol{\theta} = (\bar{\lambda}, \bar{\beta})$ is built based on the prehistoric (paleo) and historic parts of the catalogue containing only the strongest events. In this section the details of the likelihood function based on historic seismic events will be discussed, since except for a few details, the likelihood function based on prehistoric events is built in a similar manner.

By the Theorem of the Total Probability (e.g. Cramér, 1961), the probability that in time interval t either no seismic event occurs or all occurring events have a magnitude not exceeding m may be expressed as (Epstein and Lomnitz, 1966; Gan and Tung, 1983; Gibowicz and Kijko, 1994)

$$F_M^{\max}(m|m_0,t) = \sum_{i=0}^{\infty} P(i|t)[F_M(m|m_0)]^i. \tag{15}$$

Equation (15) can be expressed in a much more simpler form (e.g. Campbell, 1982) as

$$F_M^{\max}(m|m_0,t) = \left[\frac{q\lambda}{q\lambda + \bar{\lambda}_0[1 - F_M(m|m_0)]}\right]^{q\lambda t}. \tag{16}$$

In (15) and (16) is m_0 the threshold magnitude for the prehistoric or historic part of the catalogue ($m_0 \geq m_{\min}$). Magnitude $m_{\min}$ is the 'total' threshold magnitude and has a rather formal character. The only restriction on the choice of its value is that $m_{\min}$ may not exceed the threshold magnitude of any part (prehistoric, historic or complete) of the catalogue.

It follows from (16) that the probability density function (PDF) of the largest seismic event magnitude m within a period t is

$$f_M^{\max}(m|m_0,t) = \frac{q\lambda f_M(m|m_0)F_M^{\max}(m|m_0,t)}{q\lambda + \bar{\lambda}_0 t[1 - F_M(m|m_0)]}. \tag{17}$$

$\bar{\lambda}_0$ represents the mean activity rate for seismic events with magnitudes not less than m_0 and is given by

$$\bar{\lambda}_0 = \bar{\lambda}[1 - F_M(m_{min}|m_0)], \tag{18}$$

where $\bar{\lambda}$, as defined above, denotes the mean activity rate corresponding to magnitude value $m_{\min}$. Function $F_M(m|m_0)$ denotes the CDF of seismic event magnitude (13).

Based on (13) and the definition of the probability density function, it takes the form

$$f_M(m|m_{min}) = c\bar{\beta}\left(\frac{q_\beta}{q_\beta + \bar{\beta}(m - m_0)}\right)^{q_\beta + 1}. \tag{19}$$

After introducing the PDF (17) of the largest seismic event magnitude m within a period t, the likelihood function of unknown parameters $\boldsymbol{\theta}$ becomes:

$$L_0(\boldsymbol{\theta}|\boldsymbol{m_0}, \boldsymbol{t_0}, \boldsymbol{cov}) = \prod_{i=1}^{\bar{n}_0} f_{M_i^{\max}}(m_{0i}|m_0, t_i). \tag{20}$$

In order to build the likelihood function (20), three kinds of input data are required: $\boldsymbol{n_0}$, $\boldsymbol{t}$ and $\boldsymbol{cov}$. The $\boldsymbol{n_0}$ vector represents largest magnitudes, $\boldsymbol{t}$ denotes vector of the time intervals within which the largest events occurred and vector $\boldsymbol{cov} = (cov_\lambda, cov_\beta)$ consists of the coefficients of variation of the unknown parameters $\boldsymbol{\theta} = (\bar{\lambda}, \bar{\beta})$.

4.2.5. Combination of extreme and complete seismic catalogues with different levels of completeness

It is assumed that the third complete part of the catalogue can be divided into S sub-catalogues (Figure 4). Each sub-catalogue has a span T_i and is complete starting from the known magnitude $m_{\min}^{(i)}$. For each sub-catalogue i, the vector $\boldsymbol{n}_i$ denotes n_i seismic event magnitudes m_{ij}, where $m_{ij} >= m_{\min}^{(i)}$, $i = 1, \ldots, S$ and $j = 1, \ldots, n_i$. Let $\boldsymbol{L}_i(\boldsymbol{\theta}|\boldsymbol{n}_i)$ denote the likelihood function of the unknown $\boldsymbol{\theta} = (\bar{\lambda}, \bar{\beta})$, based on the i-th complete sub-catalogue. If the size of seismic events is independent of their number, the likelihood function $\boldsymbol{L}_i(\boldsymbol{\theta}|\boldsymbol{n}_i)$ is the product of two functions $L_i(\bar{\lambda}|T_i)$ and $L_i(\bar{\beta}|\boldsymbol{m}_i)$.

The assumption that the number of seismic events per unit time is distributed according to (12) means that $L_i(\bar{\lambda}|T_i)$ has the following form:

$$L^i(\bar{\lambda}|T^i) = (\bar{\lambda}^{(i)}t + q^{\lambda})^{-q^{\lambda}} \left(\frac{\bar{\lambda}^{(i)}t}{\bar{\lambda}^{(i)}t + q^{\lambda}}\right)^{n_i}, \tag{21}$$

where $\bar{\lambda}^{(i)}$ denotes the mean activity rate corresponding to the threshold magnitude $m_{\min}^{(i)}$ and is given by equation

$$\bar{\lambda}^{(i)} = \bar{\lambda}\left[1 - F^M\left(m_{\min}^{(i)} | m^{min}\right)\right]. \tag{22}$$

Following the definition of the likelihood function based on a set of independent observations and (19), $L_i(\bar{\beta}|\boldsymbol{m}_i)$ takes the form

$$L^i(\bar{\beta}|\boldsymbol{m}^i) = [c^{\beta}\bar{\beta}]^{n^i} \prod_{j=1}^{n_i} \left[1 + \frac{\bar{\beta}}{q^{\beta}}\left(m^{ij} - m_{\min}^{(i)}\right)\right]^{-(q^{\beta}+1)}. \tag{23}$$

Equations (21) and (23) define the likelihood function of the unknown parameters $\boldsymbol{\theta} = (\bar{\lambda}, \bar{\beta})$ for each complete sub-catalogue.

Finally the joint likelihood function based on all data $L(\boldsymbol{\theta})$, i.e. the likelihood function based on the whole catalogue, is calculated as the product of the likelihood functions based on prehistoric, historic and complete data.

The maximum likelihood estimates of the required hazard parameters $\boldsymbol{\theta} = (\bar{\lambda}, \bar{\beta})$, are given by the value of $\boldsymbol{\theta}$ which, for a given maximum regional magnitude $m_{\max}$, maximizes the likelihood function $L(\boldsymbol{\theta})$. The maximum of the likelihood function is obtained by solving the system of two equations $\frac{\partial \ell}{\partial \bar{\lambda}} = 0$ and $\frac{\partial \ell}{\partial \bar{\beta}} = 0$ where $\ell = \ln L(\boldsymbol{\theta})$.

A variance-covariance matrix $D(\boldsymbol{\theta})$ of the estimated hazard parameters $\hat{\bar{\lambda}}$ and $\hat{\bar{\beta}}$, is calculated according to the formula (Edwards, 1972):

$$D(\boldsymbol{\theta}) = -\begin{bmatrix} \frac{\partial^2 \ell}{\partial \bar{\lambda}^2} & \frac{\partial^2 \ell}{\partial \bar{\lambda} \partial \bar{\beta}} \\ \frac{\partial^2 \ell}{\partial \bar{\beta} \partial \bar{\lambda}} & \frac{\partial^2 \ell}{\partial \bar{\beta}^2} \end{bmatrix}^{-1} \tag{24}$$

where derivatives are calculated at the point $\bar{\lambda} = \hat{\bar{\lambda}}$ and $\bar{\beta} = \hat{\bar{\beta}}$.

4.2.6. Estimation of the region characteristic, maximum possible seismic event magnitude $m_{\max}$

Suppose that in the area of concern, within a specified time interval T, there are n main seismic events with magnitudes $m_1, \ldots, m_n$. Each magnitude $m_i \geq m_{\min}$ $(i = 1, \ldots, n)$, where $m_{\min}$ is a known threshold of completeness (i.e. all events having a magnitude greater than or equal to $m_{\min}$) are recorded. It is further assumed that the seismic event magnitudes are independent, identically distributed, random variables with CDF described by (13).

From the condition that compares the largest observed magnitude $m_{\max}^{obs}$ and the maximum expected magnitude during a specified time interval T, the maximum regional magnitude $m_{\max}$ is obtained (Kijko and Graham, 1998; Kijko, 2004)

$$m_{\max} = m_{\max}^{obs} + \frac{\delta^{1/q} \exp[n r^q/(1 - r^q)]}{\beta} \left[\Gamma(-1/q, \delta r^q) - \Gamma(-1/q, \delta)\right], \tag{25}$$

where $\delta = nC_\beta$ and $\Gamma(\cdot,\cdot)$ is the complementary incomplete Gamma function. The approximate variance of the above estimator is equal to (Kijko, 2004)

$$\sigma_{m_{\max}}^2 = \sigma_M^2 + \left\{\frac{\delta^{1/q} \exp[n r^q/(1 - r^q)]}{\beta} \left[\Gamma(-1/q, \delta r^q) - \Gamma(-1/q, \delta)\right]\right\}^2, \tag{26}$$

where σ_M is the standard error in determination of the largest observed magnitude $m_{\max}^{obs}$.

4.2.7. The Cornell-McGuire PSHA Procedure

The essence of the PSHA is the calculation of the probability of exceedance of a specified ground motion level at a specified site. The so called Cornell-McGuire solution of this problem consists of four steps: (e.g. Budnitz *et al*., 1997; Reiter, 1990):

1. Determination of the possible seismic sources around the site. The sources are typically identified faults, point sources or area sources. It is assumed that the occurrence of seismic events in these sources is spatially uniform. In the territory of eastern and southern Africa, similar to the central and eastern United States or Australia, the main contribution to the seismic hazard is attributed to the area sources. The seismicity of the area does not always correlate well with geological structures that are recognizable at the surface, making the identification of the geological structures that are responsible for seismic events difficult.

2. Determination and assessment of the recurrence parameters for each seismic source. This is typically expressed in terms of three parameters: the mean seismic activity rate λ, b-value of the Gutenberg – Richter frequency magnitude relation and the upper-bound of the seismic event magnitudes $m_{\max}$.

3. Selection of the ground motion prediction equation (GMPE), which is most suitable for the region, is crucial. For the eastern and southern Africa areas, the strong motion records are very limited therefore theoretical models of the ground motion attenuation are used. Since the ground motion attenuation relationship is a major source of uncertainty in the computed PSHA, some codes and recommendations require the use of a number of alternative GMPEs (Bernreuter *et al*., 1989).

4. Computation of the hazard curves. These curves are usually expressed in terms of the mean annual frequency of events with site ground motion level a or more, or $\lambda(a)$. Alternatively it can be expressed in terms of the probability of exceedance $P(A > a|t)$ vs. a ground motion parameter a, like PGA or a spectral acceleration.

By the Theorem of the Total Probability (Cramér, 1961), the frequency $\lambda(a)$ is defined as (Budnitz *et al*.,, 1997)

$$\lambda(a) = \sum_{i=1}^{n_S} \lambda_i \int_{m_{\min}}^{m_{\max}} \int_{R|M} P[A \geq a|M,R] f_M(m) f_{R|M}(r|m) \, dr \, dm \tag{27}$$

with subscripts i $(i = 1, \ldots, n_s)$. The seismic source number is deleted for simplicity. In (27) λ denotes the seismic source (area) characteristic, mean activity rate defined as the mean number of seismic events per time unit having magnitudes between $m_{\min}$ and $m_{\max}$. The value $m_{\min}$ is the minimum magnitude of engineering significance and $m_{\max}$ is the maximum seismic event magnitude assumed to occur on the seismic source. The probability $\Pr[A \geq a|M,R]$ denotes the conditional probability that the chosen ground motion level is exceeded for a given magnitude and distance. The standard choice for $\Pr[A \geq a|M,R]$ is the Gaussian complementary cumulative distribution function. The function is based on the assumption that the ground motion parameter a is a lognormal random (aleatory) variable. In (27) $f_M(m)$ denotes the PDF of seismic event magnitude. In most engineering applications it is assumed that seismic event magnitudes follow the Gutenberg-Richter relation. This implies that $f_M(m)$ is a negative Exponential distribution, with magnitudes between $m_{\min}$ and $m_{\max}$. If uncertainty of the seismic event magnitude distribution is taken into account then $f_M(m)$ takes the familiar compound distribution form of equation (19). Finally the PDF $f_{R|M}(r|m)$ describes the spatial distribution of seismic event occurrence or, more precisely, the PDF of the distance from the earthquake source to the site of interest. In general cases, spatial distribution of the seismic event occurrence can be different for different seismic event magnitudes.

Under the condition that seismic event occurrence in every seismic source is a Poisson event, i.e. independent in time and space, the ground motion $A \geq a$ at a site is also a Poisson event. Hence the probability that a, a specified level of ground motion at a given site, will be exceeded at least once in any time interval t is

$$P[A > a|t] = 1 - exp\left[-\sum_{i=1}^{n_S} \lambda_i \int_{m_{\min}}^{m_{\max}} \int_{R|M} P[A \geq a|M,R] f_M(m) f_{R|M}(r|m) \, dr \, dm\right]. \tag{28}$$

and is fundamental in PSHA. The plot of this equation vs. ground motion parameter a, is the hazard curve – the ultimate product of the PSHA assessment.

5. Input data

5.1 Catalogues

Reports of seismic phenomena in South Africa go back as far as 1620, to the early Dutch settlers[1)]. The seismicity is typical of an intraplate region. The natural seismic regime of a region of this type is characterised by low-level activity in terms of world standards, with seismic events randomly distributed in space and time. The correlation between most of the seismic events and the surface expression of major geological features is not clear (Fernandez and Guzman, 1979, Brandt *et al.*, 2003).

Seismic events resulting from the deep-mining operations in the gold fields of the Gauteng, Klerksdorp, Stilfontein and Welkom, form the majority of the seismic events recorded by the regional network of seismic stations (SANSN). Usually, the depth of these events varies in the range of 2-3 km below the surface.

The seismic event catalogue used in this study was compiled from several sources. After critical analysis of each of the data sources, the main contribution to pre-instrumentally recorded seismicity comes from Brandt *et al.,* (2003). The instrumentally recorded events are mainly selected from databases provided by the International Seismological Centre in UK (ISC). The ISC is a non-governmental organization charged with the final collection, analysis and publication of standard earthquake information from around the world.

The database of seismic events for South Africa is incomplete due to the fact that large parts of the country were very sparsely populated and the detection capabilities of the seismic network are far from uniform.

Unfortunately, current geological knowledge of the South African area does not provide information on all capable faults and their movements during the recent (Quaternary) geological past, especially during the last 35,000 years. There exists no known relationship between instrumentally recorded or historic seismicity and the location of faults. Also, almost no information is available on paleo-seismicity of the South African area. Therefore, in this study, the assessment of the source-

[1] It is interesting to note that the recent research by Master (2012) is questioning the credibility of the first earthquake in the South African earthquake database, event of 4 July 1620, located in Robben Island. If Master (2012) is correct, then the SA earthquake database would start from event of M_L magnitude 3.6 occurred of 15 June 1690 which took place in vicinity of today's Cape Town.

characteristic, maximum possible seismic event magnitude m_{max} (Kijko, 2004), is entirely based on knowledge of past seismicity. The other two hazard recurrence parameters (the Gutenberg-Richter b-value and the mean activity rate λ) for each seismic source has been estimated according to the procedure developed by Kijko and Sellevoll (1992). Similar to the assessment of m_{max}, the b-value and λ are based on knowledge of seismicity of the area.

The parameters of area sources λ, b-value and m_{max} were calculated for a grid size $0.1° \times 0.1°$ spanning the whole country. The seismic hazard is calculated, in the form of a matrix consisting of equally spaced grid points ($0.25° \times 0.25°$) in latitude and longitude. The area covered in this study is defined by latitudes $35°$ S to $21°$ S and longitudes $15°$ E to $33°$ E.

Following extensive analysis of the seismic event database it was established that the catalogue of the tectonic origin seismic events can be divided into eight parts, each with different level of completeness, (Table 1).

Table 1: Division of the catalogue used in the analysis.

Sub-catalogue number	Level of completeness (M_w)	Beginning of sub-catalogue	End of sub-catalogue
1	5.9	1806/01/01	1905/12/31
2	5.3	1906/01/01	1909/12/31
3	4.9	1910/01/01	1949/12/31
4	4.6	1950/01/01	1970/12/31
5	4.0	1971/01/01	1980/12/31
6	3.8	1981/01/01	1990/12/31
7	3.5	1991/01/01	1995/12/31
8	3.5	1996/01/01	2002/12/31
9	3.0	2003/01/01	2013/01/31

5.2 Ground Motion Prediction Equation (GMPE)

Attenuation is the reduction in the amplitude or energy of seismic waves caused by the physical characteristics of the transmitting media or system. It usually includes geometric effects such as the decrease in amplitude of a wave with increasing distance from the source.

Attenuation relationships, known as ground motion prediction equations (GMPEs), for South Africa were established on the basis of strong motion data that are practically non-existent (Minzi *et al*., 1999). Three attempts to establish the horizontal component of PGA attenuation for the eastern and southern Africa are published by Jonathan (1996), Twesigomwe (1997) and more recently by Mavonga (2007). Jonathan's GMPE is based on random vibration theory and is scaled by seismic records as recorded by local seismic stations. Twesigomwe's equation is a modification of the GMPE by Krinitzky *et al*., (1988). Comparison of the two regional GMPEs with the e.g. global equation by Joyner and Boore (1988), Boore *et al.*, (1993; 1994) shows relatively good agreement between regional attenuations and is used globally. Finally, the most recent GMPE by Mavonga (2007) is based on the well-known procedure of the simulation of the ground motion of large seismic events using recordings of small earthquakes (Frankel, 1995; Irikura, 1986). Seismic records of small events adjacent to the expected large events have been treated as an empirical Green's function. The advantage of the procedure is that the predicted ground motion contains information on the site response, details of path effects etc., and they can therefore often produce realistic time histories. Unfortunately, all three GMPEs are derived only for PGA and are not applicable to short distances e.g. below 10 km.

In this report the assessment of the seismic hazard for South Africa is based on the well-studied model of GMPE by Atkinson and Boore (2006). The applied GMPE was developed for the central and eastern United States which is situated in a type of tectonic environment known as an intraplate region, or equivalently, stable continental area. Because of the limited number of strong-motion records in the stable continental areas, the applied GMPE (horizontal component) has been developed mainly by help of stochastic modelling. The GMPE used in this report, including their functional form and respective coefficients are provided in Appendix A.

6. Results

Five maps of seismic hazard for South Africa were calculated. These maps are expressed in terms of peak ground acceleration (PGA). The maps indicate a 10 % probability of exceeding the PGA at least once in 50 years, for the different mean seismic activity rate correcting factors (c_f = 1, 2, 5 and 10). The correcting factor c_f is applied to the seismic activity rate λ to indicate the factor by which the activity rate is increased for the four possible scenarios i.e. a) no increase of seismicity and seismicity increases b) 2 times, c) 5 times and d) 10 times. Map No. 5 represents the estimated seismic hazard in South Africa when taking into account the four scenarios. It was assumed that the logic tree weights (l_w) of the four scenarios are 0.15, 0.50, 0.30 and 0.05 respectively. It is imported to take note that

that these weights (l_w) are very subjective; they were selected according to wide scatter and often contradicting expert opinions on the effect of hydraulic fracturing. These opinions are available in the current respective literature (e.g. Davis and Frohlich, 1993; De Pater and Baisch 2011; Davies *et al*., 2013; Green *et al*., 2012; Horton, 2012; King, 2010; Maxwell *et al*., 2009; Suckale, 2009; Zoback and Harjes, 1997) and can/will be modified as more seismological effects of eventual future hydraulic fracturing will become known.

Comparison of these five maps suggest that the introduction of hydraulic fracturing in South Africa can/will lead to high levels of seismic hazard in the parts of the Western Cape, the Free State, Gauteng and towards the eastern border of the North West Province. Moderate hazard levels can be expected in the Limpopo Province and parts of the Northern Cape. The southern part of the Eastern Cape is subject to low levels of seismic hazard.

A more reliable assessment of effect of hydraulic fracturing on seismic hazard in South Africa can be achieved only through the inclusion of detailed geological and tectonic information about the area.

6.1 Seismicity

Maps No. 1 to 5 indicate a wide range of accelerations which are represented by the colours white to maroon. The accelerations range from 0.01 g to 0.14 g and is grouped together as indicated in Table 2. The classifications were done based on the current seismic activity for South Africa (Map No. 1) and applied to Maps No. 2 to 5, which represents the hypothetical increased activity rate that could possibly be attributed to hydraulic fracturing.

Table 2: Classification of acceleration range for mapping purposes

Hazard Classification	Acceleration Range	Colour Code
No Hazard	0.0 g	White
Low Hazard	0.0 g - 0.05 g	Green
Moderate Hazard	0.05 g – 0.0875 g	Yellow
High Hazard	0.0875 g – 0.125 g	Pink
Very High Hazard	> 0.125 g	Maroon

The highest expected accelerations for each of the respective seismic hazard maps of PGA is 0.14 g ($c_f = 1$), 0.17 g ($c_f = 2$), 0.25 g ($c_f = 5$), 0.34 g ($c_f = 10$) and 0.24 resulting from the application of the logic tree formalism. The map with the highest level of hazard is Map No. 4 ($c_f = 10$), with peak ground accelerations in the region of 0.18 to 0.3 g in the north-eastern part of South Africa (parts of Mpumalanga, Gauteng, North West Province, Free State, Lesotho, KwaZulu Natal and Swaziland). High PGA accelerations (order of 0.2 to 0.4 g) are indicated by the maps for the south-western part of the Western Cape. It is important to note that although by international norms the expected seismic hazard is not high, it is still high enough to cause significant damage to infrastructure.

A common trend between in Maps No. 1 to 5 (within their respective ranges) is the high level of hazard in parts of the Western Cape, the Free State, Gauteng and the eastern parts of the North West Province. Moderate hazard levels can be seen in the Limpopo Province and parts of the Northern Cape. Low levels of hazard can be seen in the southern part of the Eastern Cape.

The PGA map (Map No. 1) gives comparable results compared to the most recent seismic hazard map of Southern Africa (Kijko *et al.*, 2003), which is implemented into the South African Building Code 2009 (SABS, 2009). The three maps, Maps No. 2-4, yield the following expected hazard levels: in terms of natural seismic activity there is a high expected level of hazard (about 0.2 g) in the south-Western Cape. Moderate hazard levels, in the order of 0.1 g, are expected in Lesotho and low levels (0.05 g) of hazard are expected in the southern region of the Eastern Cape. In terms of mining-induced seismicity; the highest expected peak ground accelerations, in the order of 0.2 g, can occur in the Free State and Gauteng mines. Moderate hazard levels of 0.1 g are predicted for KwaZulu Natal.

6.2 Possible Effect of Hydraulic Fracturing

Not enough research have been performed to allow the researchers to release a categorical statement in terms of which areas can be classified as safe or not safe in terms of hydraulic fracturing. The seismicity for South Africa is not equally well documented for different areas in the country, for instance the Karoo area. This is mainly due to the low density of seismometers in the South African National Seismological Network (SANSN). A very limited number of stations are not capable to detect weak seismic events. Buried faults can therefore go undetected. The establishment of a local seismic network before hydraulic fracturing starts is fundamentally important to ensure that no drilling occurs on or near any faults or areas of tectonic stress concentrations. The use of the current

knowledge of the local geology in this respect could also be extremely helpful in the absence of instrumental observations.

The local tectonic conditions are crucial indicators needed to determine the level of increase of seismicity in an area. These conditions include the local geological make-up, buried faults, local seismotectonics (which can be established by seismic tomography) and tectonic stresses. The history of the seismic activity in the area is also an important factor which, up to large extend, determines the seismicity induced by a process such a hydraulic fracturing.

6.3 Seismicity Maps

The seismic hazard maps for South Africa in terms of peak ground acceleration (PGA) are provided below. The maps respectively indicate a 10 % probability of exceeding the calculated PGA at least once in 50 years for the different increased activity rate correcting factors (c_f = 1, 2, 5 and 10), as well as the combination of these scenarios through a logic tree.

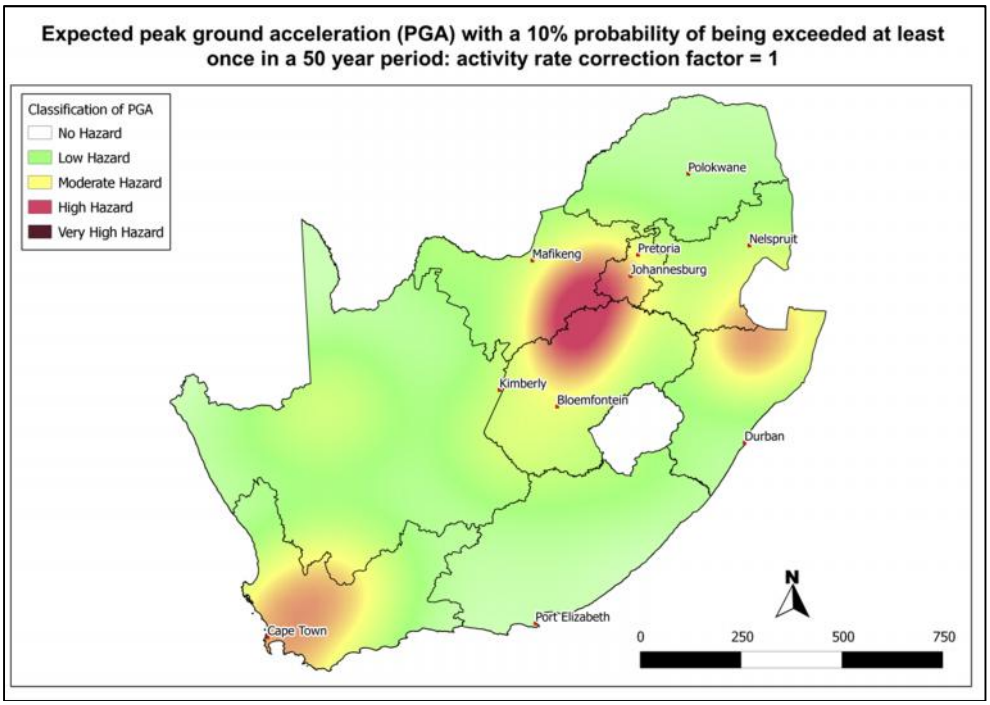

Map No. 1: Map of current seismic hazard for South Africa (applied correcting factor of the activity rate c_f = 1). This map shows the expected PGA with a 10 % probability of being exceeded at least once in a 50 year period.

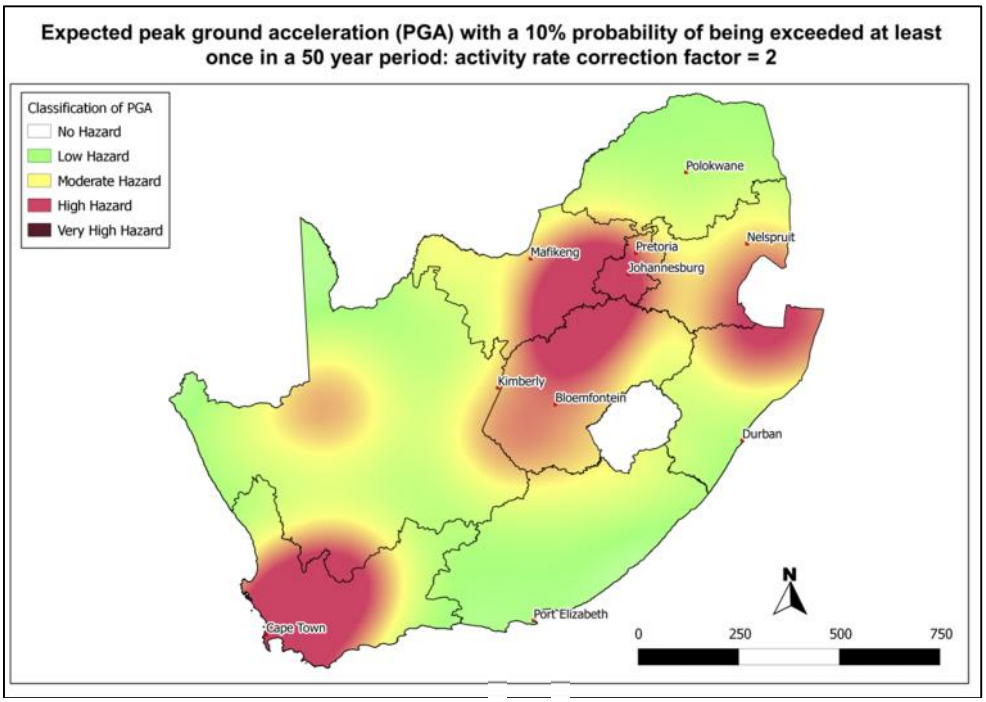

Map No. 2: Map of the expected PGA with a 10 % probability of being exceeded at least once in a 50 year period with the applied activity rate correcting factor $\boldsymbol{c_f = 2}$.

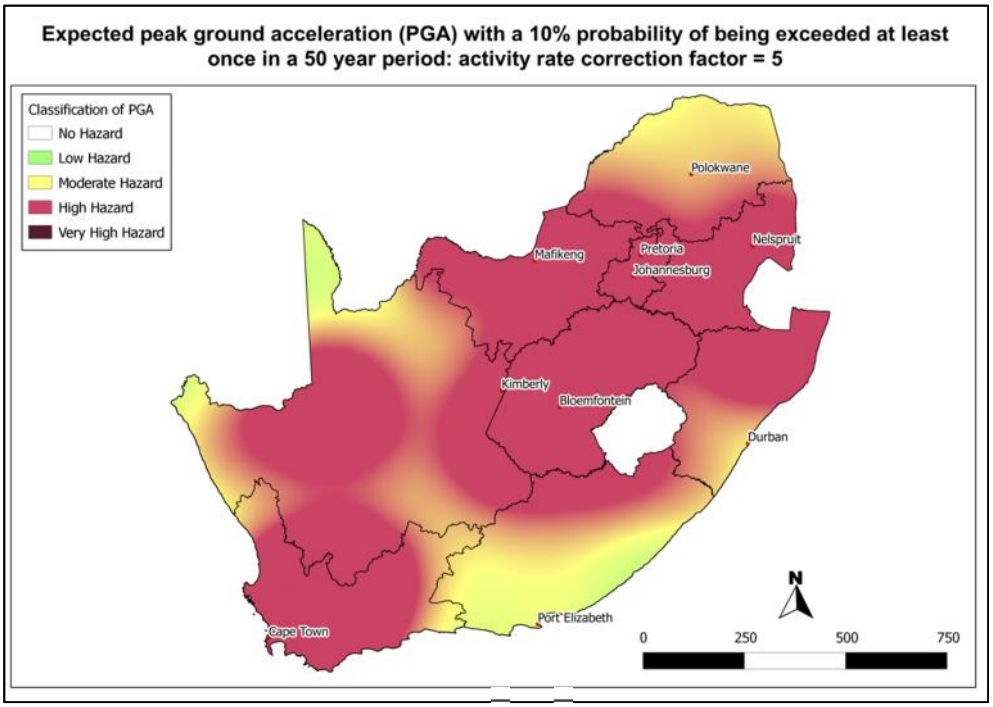

Map No. 3: Map of the expected PGA with a 10 % probability of being exceeded at least once in a 50 year period with the applied activity rate correcting factor $\boldsymbol{c_f = 5}$.

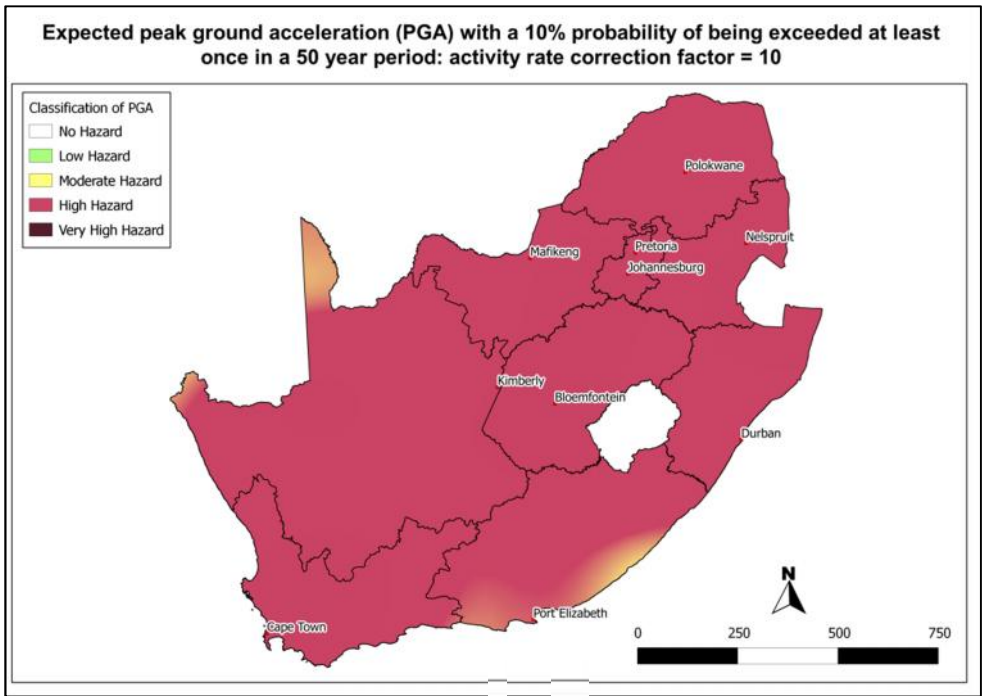

Map No. 4: Map of the expected PGA with a 10 % probability of being exceeded at least once in a 50 year period with the applied activity rate correcting factor $\boldsymbol{c_f = 10}$.

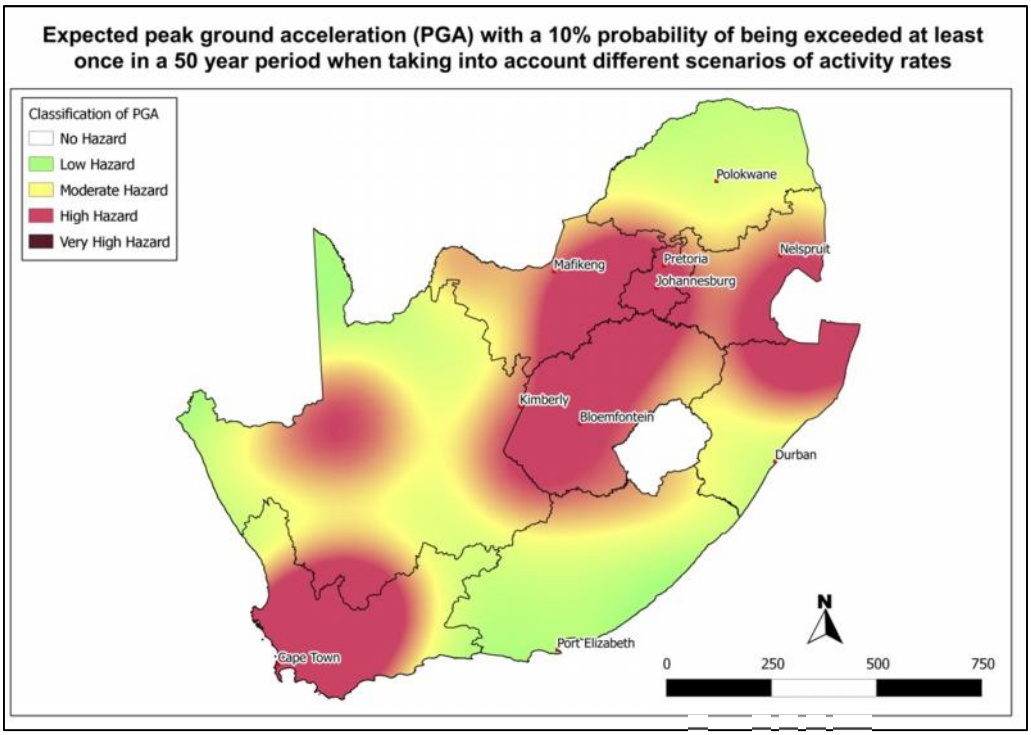

Map No. 5: Map of the expected PGA with a 10 % probability of being exceeded at least once in a 50 year period taking into account all the possible scenarios for activity rate ($\boldsymbol{c_f = 1, 2, 5, 10}$).

For the purpose of this report the associated hazard (peak ground acceleration) is set equivalent to vulnerability as defined in UNISDR (2004). This report defines vulnerability as the conditions determined by physical, social, economic and environmental factors or processes, which increase the susceptibility of a community to the impact of hazards.

7. Monitoring Protocol

In comparison with global seismicity southern Africa is one of the most stable regions of the Earth. However, it is not completely deprived of seismic activity. An unusual aspect in the seismicity of South Africa is that most of the recorded seismic activity is associated with the deep gold mining operations on the periphery of the Witwatersrand Basin. Natural, low magnitude earthquakes occur sporadically over time and space, portraying typical intraplate seismicity.

Owing to the relatively short documented seismic history of the southern African sub-continent most of the available information relates to instrumental data acquired since 1971. Most of the information regarding pre-1971 events is based on macro-seismic observations. Consequently, the locations of these events correspond, in most cases, to the sites where the seismic event was felt with maximum intensity but may be displaced by tens of kilometres from the true epicentre.

The database of seismic information for South Africa is evidently incomplete, especially for the historic part of the seismic event catalogue. The completeness could be estimated by comparing the apparent frequency of occurrence of events with pre-assumed frequency-magnitude relationships (Shapira *et al*., 1989; Saunders *et al*., 2008).

Although the situation has improved since 1989 through the deployment of more seismic stations, the overall threshold for determining the magnitude for both the tectonic origin and mine related seismic events is still around magnitude M_w 3.0.

International regulatory guides clearly states that any study related to the siting, rating and development of critical engineering structures must include seismic monitoring as one of the components. It is therefore imperative that the collection and monitoring of data should start well in advance before any exploration is undertaken on the site, and should continue well after hydraulic fracturing has ceased in the area. The only means to comply with international standards of identifying if an area is capable of generating seismic events is to, as in the case of mining induced

seismicity or tectonic active (capable) faults, install a local seismic network with the capability of recording micro-seismic events with Richter magnitudes, say less than 1.0.

Knowledge of micro-seismic events provides knowledge about large, potentially dangerous events in the future through the extrapolation of the rate of occurrence of small events to larger events. In South Africa, knowledge about micro-seismicity is virtually the only information available, since the occurrence of large events is very rare. The analysis of micro-seismic event records provides useful data of engineering significance. In order to provide sufficient coverage over the epicentre location for the area of interest, it is recommended that an area with a radius of ca. 100 km, from the hydraulic fracturing site, be monitored. This local micro-network links the hydraulic fracturing operations with seismic data processing and data interpretation for meaningful interpretation of events as they unfold. The network should also report to the regional and/or national seismic networks.

Seismic monitoring before exploration will aid in identifying the location of faults and the stress field nature in areas where it is currently unknown. Although most faults are inactive and does not pose a potential problem, it assists in the seismic characterization of the site (Cook et al., 2013). This is necessary in the establishment of a baseline and should therefore be done before the hydraulic fracturing process begins.

In certain cases e.g. when hydraulic fracturing will take place in vicinity of known tectonic faults or significant infrastructure, it would be advantageous to install, in addition to a local seismograph network, several strong motion accelerographs. The recorded seismic events should be carefully studied and, if possible, linked with the local tectonics of the area.

Detailed information on seismicity is therefore needed in order to obtain meaningful information about the potential increase in seismicity associated with hydraulic fracturing. It is recommended that a network of seismographs and accelerographs, that have the ability to record macro- and micro-earthquakes, be installed and operated before and during exploration as well as during and after mining. It is strongly recommended to begin this seismic monitoring before the hydraulic fracturing exploration phase in order to establish a baseline.

Data Management

The establishment and management of the recommended local seismic network to ensure data integrity, is if upmost importance. The number of sensors and their configuration in this local seismic network should be arranged such that it provides the required location of the seismic event epicentres

with an accuracy of a few 100 meters. To obtain this required accuracy, the network optimization should be done before the instalment of the seismic network (see e.g. Kijko, 1997a and b).

Currently the Council for Geoscience (CGS) maintain the South African National Seismograph Network (national and regional networks). The database maintained by the CGS can be viewed as the most up to date data archive on seismic activity in South Africa. Investigations should be made to determine if the existing system can be effectively adapted to manage seismic information at oil and gas well sites, or if a new local networks should be established.

If the CGS is not capable of providing the necessary support, an independent entity would have to establish, manage, analyse and disseminate the relevant networks and information.

8. Disclaimer

Neither the University of Pretoria Natural Hazard Centre, Africa nor any other party involved in creating, producing or delivering the report shall be liable for any direct, incidental, consequential, indirect or punitive damages arising out of the misuse of the information contained in this report. The University of Pretoria Natural Hazard Centre, Africa does not guarantee the accuracy of information provided by external sources and accepts no responsibility or liability for any consequences arising from the use or misuse of such data.

9. References

Aki, K., (1965). Maximum likelihood estimate of *b* in the formula log N = a – b·M and its confidence limits, *Bull. Earthq. Res. Inst.*, Univ Tokyo ***47*****,** 237-239**.**

Atkinson, G.M. Boore, D.M., (2006). Earthquake ground-motion prediction equations for Eastern North America. *Bull. Seism. Soc. Am*. **96**, 2181-2205.

AXCO (unpublished). Insurance Market Report on South Africa – Non-Life, AXCO

Benjamin, J.R. (1968). Probabilistic models for seismic forces design, *J. Struct. Div., ASCE* **94**, (ST5) 1175-1196.

Bernreuter, D.L., Savy, J.B., Mensing, R.W., Chen, J.C., (1989). *Seismic Hazard Characterization of 69 Nuclear Plant Sites East of the Rocky Mountains*. Report NUREG/CR-5250, vols 1-8, prepared by Lawrence Livermore National Laboratory for the U.S. Nuclear Regulatory Commission.

Boore, D. M., Joyner, W. B., Fumal, T.E., (1994). Estimation of response spectra and peak accelerations from western North American earthquakes: An interim report, Part 2, *U.S. Geological Survey Open-File Report 94-127*}.

Boore, D. M., Joyner, W. B., Fumal, T.E., (1993). Estimation of response spectra and peak accelerations from western North American earthquakes: An interim report, *U.S. Geological Survey Open-File Report 93-509*} 72 pp.

Brandt, M.B.C., Saunders, I., Graham, G., (2003). Frequency-magnitude relationship and estimated m_{max} from micro-seismic data, and regional- and historical data sets for the Southern part of South Africa, Africa Geoscience Review.

Budnitz, R.J., Apostolakis, G., Boore, D.M., Cluff, L.S., Coppersmith, K.J., Cornell, C.A., Morris, P.A., (1997). *Recommendations for Probabilistic Seismic Hazard Analysis: Guidance on Uncertainty and Use of Experts.* NUREG/CR-6372, UCR-ID-122160, Main Report 1. Prepared for Lawrence Livermore National Laboratory.

Campbell, K.W. (1982). Bayesian analysis of extreme earthquake occurrences. Part I. Probabilistic hazard model, *Bull. Seism. Soc. Am*., **72**, 1689-1705.

Campbell, K.W. (1983). Bayesian analysis of extreme earthquake occurrences. Part II. Application to the San Jacinto Fault zone of southern California, *Bull. Seism. Soc. Am*., **73**, 1099-1115.

Cook, P., Beck, V., Brereton, D., Clark, R., Fisher, B., Kentish, S., Toomey, J., Williams, J. (2013) *Engineering Energy: unconventional gas production.* Report for the Australian Council of Learned Academics, www.acola.org.au.

Cornell, C.A., (1968). Engineering seismic risk analysis, *Bull. Seism. Soc. Am*. **58**, 1583-1606.

Cramér, H., (1961). *Mathematical Methods of Statistics*, Princeton University Press Princeton.

Davis, S.D., Frohlich, C. (1993). Did (or will) fluid injection cause earthquakes?: Criteria for a rational assessment, *Seismological Research Letters* **64**, 207–224.

Davies, R., Foulger, G., Bindley, A., Styles, P. (2013). Induced seismicity and hydraulic fracturing for the recovery of hydrocarbons, *Marine and petroleum geology*, (in print), 60p. http://www.sciencedirect.com/science/journal/02648172.

Dennison, P.I.G. van Aswegen, G., (1993). Stress modelling and seismicity on the Tanton fault: A case study in a South African gold mine. *In* "Rockbursts and Seismicity in Mines" (R.P. Young, ed.). Balkema, Rotterdam, pp. 327 – 335.

De Pater C.J., Baisch, S. (2011). *Geomechanical Study of Bowland Shale Seismicity*. Synthesis Report. StrataGen Delft BV, Q-con GmbH. 71p.

Edwards, A.W.F., (1972). *Likelihood*, Cambridge University Press, New York, p. 235.

Epstein, B., Lomnitz, C., (1966). A model for occurrence of large earthquakes, *Nature*, **211**, 954-956.

Fernandez, L.M., Guzman, J.A., (1979a). Earthquake hazard in Southern Africa. *Seismologic series No* **10**. Geological Survey of South Africa. 22 pp.

Fernandez, L.M., Guzman, J.A. (1979b). Seismic History of Southern Africa, Geological Survey of South Africa, *Seismologic Series* **9**, pp. 1-38.

Fernandez, L.M., du Plessis, A., (1992). Seismic Hazard Maps for Southern Africa. Council for Geoscience.

Frankel, A., (1995). Simulating strong motions of large earthquakes using recordings of small earthquakes. *Bull. Seism. Soc. Am.*, **85**, 1144-1160.

Gan, Z.J., Tung, C.C., (1983). Extreme value distribution of earthquake magnitude, *Phys. Earth Planet. Inter.* **32**, 325-330.

Gibowicz, S.J., Kijko, A., (1994). *An Introduction to Mining Seismology*, Academic Press, San Diego.

Gibowicz, S. J., Lasocki, S., (2001). Seismicity induced by mining: ten years later. *Advances in Geophysics*, vol. **44**, 39 – 181.

Gordon, R.G., Stein, S. (1992). Global tectonics and space geodesy. *Science*. **256**. 333-342.

Grand, S.P., Van der Hilst, R.D.. Widiyantoro, S., (1997). Global seismic tomography: A snapshot of convection in the Earth. *Geological Society of America Today*. **7**. 4. 1-7.

Green, C.A., Styles, P., Baptie, B.J. (2012). Preese Hall shale gas fracturing review and recommendations for induced seismic mitigation. http://www.decc.gov.uk/assets/decc/11/ meeting energy demand/oil-gas/5055 preese hall shale gas fracturing review and recomm.pdf.

Hamada, M.S., A.G. Wilson, C. Shane Reese and H.F. Martz (2008). *Bayesian Reliability*, Springer, New York, pp.430.

Hartnady, C.J.H., Partridge, T.C., (1995). Neotectonic uplift in southern Africa: A brief review and geodynamic conjecture. Proceedings of the Centennial Geo congress of the Geological Society of South Africa. **1**. 456-459.

Horton, S. (2012). Disposal of hydrofracking waste fluid by injection into subsurface aquifers triggers earthquake swarm in Central Arkansas with potential for damaging earthquake, *Seismological Research Letters*, **83,** 250-260**.**

Irikura, K., (1986). Prediction of strong acceleration motions using empirical Green's function, Proc.7th Japan Conf. Earthquake Engineering, 151- 156.

International Seismological Centre, On-line Bulletin, http://www.isc.ac.uk, Internatl. Seis. Cent., Thatcham, United Kingdom, 2010.

Jonathan, E., (1996). *Some aspects of seismicity in Zimbabwe and Eastern and Southern Africa.* M. Sc. Thesis Institute of Solid Earth Physics, Bergen University, Bergen, Norway, pp.100.

Joyner, W.B., Boore, D., (1988). Measurement, characterization and prediction of strong ground motions, in: Von Thun, J.L. (ed.), Proc. Conference Earthquake Engineering and Soil Dynamics II, Recent Advances and Ground Motion Evaluation, Park City, Utah, ASCE Geotechnical Special Publication No. 20, pp. 43-102.

Kijko, A (1977a) An algorithm for the Optimum Distribution of a Regional Seismic Network - I. *Pageoph*, Vol 115, pp. 999-1009

Kijko, A (1977b) An algorithm for the Optimum Distribution of a Regional Seismic Network - II. An analysis of the Accuracy of Location of Local Earthquakes Depending on the Number of Seismic Stations, *Pageoph*, Vol 115

Kijko**,** A., (2004). Estimation of the maximum earthquake magnitude m_{max}. *Pure Appl. Geophys*, 161, 1-27.

Kijko, A. Graham, G., (1998). "Parametric-Historic" procedure for probabilistic seismic hazard analysis. Part I: Assessment of maximum regional magnitude m_{max}, *Pure Appl. Geophys*, **152**, 413-442.

Kijko, A., Sellevoll, M.A. (1989). Estimation of earthquake hazard parameters from incomplete data files, Part I, Utilization of extreme and complete catalogues with different threshold magnitudes. *Bull. Seism. Soc. Am.* **79**, 645-654.

Kijko, A. Sellevoll, M.A., (1992). Estimation of earthquake hazard parameters from incomplete data files. Part II. Incorporation of magnitude heterogeneity. *Bull. Seism. Soc. Am.* **82**, 120-134.

Kijko, A., Retief, S.J.P., Graham, G., (2003). Seismic Hazard and Risk Assessment for Tulbagh, South Africa: Part II – Assessment of Seismic Risk. *Natural Hazards*, **30**, 25-41

King, G.E. (2010). Thirty Years of Shale Gas Fracturing: What Have We Learned? SPE 119896.

Klugman, S.A., H.H. Panjer, and G.E. Willmot (2008). *Loss Models. From Data to Decisions*, John Willey & Sons, Inc., Hoboken, New Jersey, pp.726.

Krinitzky, E.L., Chang, F.K., Nuttli, O.W., (1988). Magnitude related earthquake ground motion. *Bull. Ass. Eng. Geol.*, **25,** 399-423.

Lemaux, J., Gordon, R.G. Royer, J., (2002). Location of the Nubia-Somalia boundary along the Southwest Indian Ridge. *Geology*. **30**. 339-342.

Master, S., (2012). Oldest 'earthquake' in South Africa (Robben Island, 07 April 1620) discredited. S Afr. J Sci. 2012;108(9/10), Art. #975, 3 pages. http:// dx.doi.org/10.4102/sajs. v108i9/10.975

Mavonga, T., (2007). An estimate of the attenuation relationship for the strong ground motion in the Kivu Province, Western Rift Valley of Africa, *Phys. Earth Planet. Interiors*, **162**, 13-21.

Maxwell, S.C., Jones, M., Parker, R., Miong, S., Leaney, S., Dorval, D., D'Amico, D., Logel, J., Anderson, E., Hammermaster, K. (2009). Fault Activation During Hydraulic Fracturing SEG Houston 2009 International Exposition and Annual Meeting 1552-1556.

Microscopic and Macroscopic Simulation: Towards Predictive Modelling of the Earthquake Process, Editors: P. Mora, Matsu'ura, M., Madariaga, R., Minster, J-B., *Pure and Applied Geophysics*, **157**, pp. 1817-2383, 2000.

Minzi, V, Hlatywayo, D.J., Chapola, L.S., Kebeda, F., Atakan, K., Kebede, F., Atakan, K., Lombe, D.K., Turyomurugyendo, G. Tugume, F.A., (1999). Seismic Hazard Assessment in Eastern and Southern Africa. *Annali di Geofisica*, **42**, 1067-1083.

Nyblade, A.A. Robinson, S.W., (1994). The African superswell. *Geophysical Research Letters*. **21**. 9. 765-768.

Reiter, L., (1990). *Earthquake Hazard Analysis: Issues and Insight*, Columbia University Press, New York.

SABS, (1994). South African Standard Code of Practice for The general procedures and loadings to be adopted in the design of buildings. SABS 0160:1989 (Amended 1990, 1991, 1994)

SABS (2009). South African National Standard Basis of structural design and actions for building and industrial structures Part 4: Seismic actions and general requirements for building, 2009. SANS 10160-4 (2009). Edition 1.

Saunders, I., Brandt, M., Steyn, J., Roblin, D., Kijko, A., (2008). The South African National Seismograph Network. *Seismol. Research Letters*, **79**, Number 2, 203-210.

Seismicity Patterns, their Statistical Significance and Physical Meaning, Editors: Wyss, M., Shimazaki, K., A. Ito, A., *Pure and Applied Geophysics*, **155**, pp. 203-726, 1999

Simpson, D.W., Richards, P.G., (1981). *Earthquake Prediction, An International Review.* Maurice Ewing series IV, Eds: D. W. Simpson, P.G. Richards. American Geophysical Union, Washington, D.C., 680 pp.

Shapira, A., Fernandez, L.M. and Du Plessis, A. (1989). Frequency-magnitude relationships of southern African seismicity. *Tectonophysics*, 261 – 271

Su, W., Woodward, R.L. Dziewonski, A.M., (1994). Degree 12 model of shear velocity heterogeneity in the mantle. *Journal of Geophysical Research*. **99**. 6945-6980.

Suckale, J., (2009). Induced seismicity in hydrocarbon fields, *Advances in Geophysics*, **51**, Chapter 2, 55-106.

Twesigomwe, E., (1997). *Probabilistic seismic hazard assessment of Uganda.* Ph.D. Thesis, Makarere University, Uganda.

UNISDR. (2004). International Strategy for Disaster Reduction. Retrieved 2011 йил 28-March from International Strategy for Disaster Reduction.: http://www.unisdr.org/eng/library/lib-terminology-eng%20home.htm.

Van Wyk, W.L., Kent, L.E., (1974). The Earthquake of 29 September 1969 in the Southwestern Cape Province, South Africa. *Geological Survey of South Africa*, Seismologic Series 4: 53pp

Wong, I.G., (1993). Tectonic stresses in mine seismicity: Are they significant? *In* "Rockbursts and Seismicity in Mines" (R.P. Young, ed.). Balkema, Rotterdam, pp. 273 – 278.

Zoback, M.D., Harjes, H-P. (1997). Injection-induced earthquakes and crustal stress at 9 km depth. *Journal of Geophysical Research* **102**, 18,477-18,491.

Appendix A

Applied Ground Motion Prediction Equation

ATKINSON-BOORE (BSSA, vol.96, pp.2181-2205, 2006)

ln[a(f)] = c1 + c2*mag + c3*mag^2 + (c4 + c5*mag)*f1 + (c6 + c7*mag)*f2 +(c8 + c9*mag)*f0 + c10*r + p*SD

WHERE:

a = MEDIAN VALUE, HARD ROCK, AVERAGE HORIZONTAL COMPONENT PGA/ARS [g]
f = GROUND MOTION FREQUENCY. IF a = PGA, f = 99.9 [Hz]
mag = EARTHQUAKE MAGNITUDE Mw
r = HYPOCENTRAL DISTANCE (CLOSEST DISTANCE TO THE FAULT) [KM]
f0 = MAX[log10(r0/r),0], r0 = 10 KM
f1 = MIN[log10(r/r1), r1 = 70 KM
f2 = MAX[log10(r/r2),0], r2 = 140 KM
p = 0. IF p = 1, ln(a) = MEAN[ln(a)] + SD[ln(a)]
c1,...,c10 = COEFFICIENTS; SD OF PREDICTED ln(a) = 0.69

ATTENUATION COEFFICIENTS

Freq.(Hz)	c1	c2	c3	c4	c5	c6	c7	c8	c9	c10
0.2	-5.41	1.710	-0.0901	-2.54	0.227	-1.270	0.116	0.979	-0.1770	-0.0002
0.3	-5.79	1.920	-0.1070	-2.44	0.211	-1.160	0.102	1.010	-0.1820	-0.0002
0.4	-6.17	2.210	-0.1350	-2.30	0.190	-0.986	0.079	0.968	-0.1770	-0.0003
0.5	-6.18	2.300	-0.1440	-2.22	0.177	-0.937	0.071	0.952	-0.1770	-0.0003
0.8	-5.72	2.320	-0.1510	-2.10	0.157	-0.820	0.052	0.856	-0.1660	-0.0004
1.0	-5.27	2.260	-0.1480	-2.07	0.150	-0.813	0.047	0.826	-0.1620	-0.0005
2.0	-3.22	1.830	-0.1200	-2.02	0.134	-0.813	0.044	0.884	-0.1750	-0.0008
2.5	-2.44	1.650	-0.1080	-2.05	0.136	-0.843	0.045	0.739	-0.1560	-0.0009
4.0	-1.12	1.340	-0.0872	-2.08	0.135	-0.971	0.056	0.614	0.1430	-0.0011
5.0	-0.61	1.230	-0.0789	-2.09	0.131	-1.120	0.068	0.606	-0.1460	-0.0011
8.0	0.21	1.050	-0.0666	-2.15	0.130	-1.610	0.105	0.427	-0.1300	-0.0012
10.0	0.48	1.020	-0.0640	-2.20	0.127	-2.010	0.133	0.337	-0.1270	-0.0010
20.0	1.11	0.972	-0.0620	-2.47	0.128	-3.390	0.214	-0.139	-0.0984	-0.0003
25.2	1.26	0.968	-0.0623	-2.58	0.132	-3.640	0.228	-0.351	-0.0813	-0.0001
40.0	1.52	0.960	-0.0635	-2.81	0.146	-3.650	0.236	-0.654	-0.0550	-0.0000
PGA	0.91	0.983	-0.0660	-2.70	0.159	-2.800	0.212	-0.301	-0.0653	-0.0004

Appendix B

Seismicity and Hydraulic Fracturing

(Water Research Commission Project K5/2149: Development of an interactive vulnerability map and preliminary screening level monitoring protocol to assess the potential environmental impact of hydraulic fracturing: Background review report, 2013)

Impacts

Already in the 1920s it became clear that pumping fluids into or out of the Earth can cause strong seismic events (NRC, 2012). Some of them can be strong enough to cause damage. In seismological literature, these events are known as man-made or induced earthquakes.

The most memorable and well documented example of an induced seismic related event due to fluid injection is the induced seismicity that occurred in the Denver, Colorado area in the 1960s. An injection of liquid waste disposal at the Rocky Mountain Arsenal into impermeable crystalline basement rock caused several seismic events with magnitudes within a range of 5.0 to 5.5. The largest event caused damage estimated in 1967 of US $500,000 (Healy *et al*., 1968; Nicholson and Wesson, 1990).

More recent examples of induced seismicity caused by pumping fluids into or out of the rock include seismic events in Basel, Switzerland, as well as in Arkansas, Ohio and Oklahoma, Texas in the USA (Frohlich *et al.*, 2011; Horton and Ausbrooks, 2010 and 2011, Horton, 2012). For example (Kerr, 2012), during extensive fluid injection in the vicinity of the town of Guy, Arkansas, a magnitude 4.0 event struck about a kilometre northeast of the two fracturing wells. Ten days later, a magnitude 3.9 event took place, ca. two kilometres farther to the northeast toward Guy. Two months later, two events of magnitude 4.1 and 4.7 took place to the southwest of the deeper well, towards the town of Greenbrier. In March 2011, the Ohio Department of Natural Resources announced that it had evidence “strongly indicating” that wastewater injection - at least part of it used for fracturing purposes - had triggered several magnitude 2.0 to 4.0 seismic events in the town of Youngstown. In 2001, seismic activity was observed along the Colorado–New Mexico border, the place where drillers were injecting water to extract methane from coal beds. In central and southern Oklahoma, seismicity increased in 2009 by a factor of 20 over the rate of the previous half-century, even when the

November's magnitude 5.6 and its aftershocks are excluded from the calculation (Ake *et al*., 2005; Holland and Gibson, 2011).

It is not always is clear what is the cause of this strong induced seismicity (Zoback *et al*, 2010). Dr. Mark Zoback of Stanford University in Palo Alto, California is pointing out that there are already 144,000 wastewater injection wells in the country, but very few are generating seismic events. Injection of fluid in rocks causes an increase of the pore pressure and also modifies the state of the stress (NRC, 1990; Hsieh and Bredehoeft, 1996). The stress change is associated with a volume expansion of the rock due to the increase of the pore pressure. However, the pore pressure perturbation dominates over the stress variation and when considering the consequence of fluid injection with regard to the induced seismicity, the stress perturbations can often be ignored.

In assessing the potential for induced seismicity, two basic questions arise: (1) what is the magnitude of the pore pressure change and (2) what is the extent of the volume of rock where the pore pressure is modified in any significant manner. Current understanding is that the magnitude of the induced pore pressure increase and the extent of the region of pore pressure change depend on the rate of fluid injection, total volume injected, the fluid viscosity and as well as hydraulic properties of the rock, its intrinsic permeability and its storage coefficient (e.g. Shapiro and Dinske, 2009).

Can we control the occurrence of strong seismic events induced by fluid injection? According to Dr Zoback, one has to "look before you leap". He believes that the seismic tomography techniques should be employed to locate buried faults capable of generating strong seismic events, up to magnitude 6.0 (Zoback and Townend, 2001; Zoback *et al*., 2010).

In addition, at the beginning of the injection, the surrounding area should be monitored by a network of seismometers. The monitoring and data analysis should be done in real time. It will allow researchers to produce an image of the subsurface and to identify the potential area of location for strong seismic events. Such "hot spots" must be avoided during hydraulic fracturing.

Reference

Ake, J., K. Mahrer, K., O'Connell, D., Block, L., (2005). Deep-injection and closely monitored induced seismicity at Paradox Valley, Colorado. *Bulletin of the Seismological Society of America* 95, 664– 683.

Frohlich, C., Hayward, C., Stump, B., Potter, E., (2011). The Dallas–Fort Worth earthquake sequence: October 2008 through May 2009. *Bulletin of the Seismological Society of America* 101, 327–340.

Healy, J. T., Rubey, W.W., Griggs, D.T., Raleigh, C.B., (1968). The Denver earthquakes. *Science* 161, 1,301–1,310.

Holland, A., Gibson, A.R., (2011). Analysis of the Jones, Oklahoma, earthquake swarm. *Seismological Research Letters* 82, 279 (abstract)

Horton, S., Ausbrooks, S.M., (2010). Are recent earthquakes near Greenbrier, Arkansas, induced by waste-water injection? *Seismological Research Letters* 81, 378 (abstract).

Horton, S., Ausbrooks, S.M., (2011). Possible induced earthquakes in central Arkansas. *Seismological Research Letters* 82, 279 (abstract).

Horton, S. (2012). Disposal of Hydrofracking Waste Fluid by Injection into Subsurface Aquifers Triggers Earthquake Swarm in Central Arkansas with Potential for Damaging Earthquake, *Seismological Research Letters* Volume 83, Number 2 March/April 2012. 250-260.

Hsieh, P.A., Bredehoeft, J.S., (1996). *A reservoir analysis of the Denver earthquakes: A case of induced seismicity*. Journal of Geophysical Research 86(B2): 903-920.

Kerr, R., (2012). Learning how to NOT make your own earthquakes. *Science* 335: 1436-1437.

Nicholson, C., Wesson, R.L., (1990). *Earthquake hazard associated with deep well injection: A report to the U.S. Environmental Protection Agency*. Reston, VA: U.S. Geological Survey Bulletin 1951, 74 p.

NRC (National Research Council), (1990). *The Role of Fluids in Crustal Processes*. Washington, DC: National Academy Press.

NRC (2012). *Induced Seismicity Potential in Energy. Technologies*. The National Research Council. Committee on Induced Seismicity Potential in Energy Technologies Committee on Earth Resources, Committee on Geological and Geotechnical Engineering, Committee on Seismology and Geodynamics Board on Earth Sciences and Resources, Division on Earth and Life Studies. The National Academies Press, Washington D.C, 240 p.

Shapiro S.A. Dinske, C., (2009). Fluid-induced seismicity: Pressure diffusion and hydraulic fracturing, *Geophysical Prospecting*, 2009, 57, 301–310 doi: 10.1111/j.1365-2478.2008.00770.x

Zoback, M. D., Townend, J., (2001). Implications of hydrostatic pore pressures and high crustal strength for the deformation of intraplate lithosphere. *Tectonophysics* 336, 19–30.

Zoback M, Kitasei, S. Copithorne, B., (2010). *Addressing the Environmental Risks from Shale Gas Development (briefing paper 1).* Worldwatch Institute. Washington, DC. 18 pp.